ELSEVIER

Two-dimensional simulation of water flow and solute transport below furrows: model calibration and validation

Fariborz Abbasi[a], Jan Feyen[a,*], M.Th. van Genuchten[b,1]

[a]*Institute for Land and Water Management, Katholieke Universiteit Leuven, Vital Decosterstraat 102, 3000 Leuven, Belgium*
[b]*George E. Brown Jr., Salinity Laboratory, USDA-ARS, 450 W. Big Springs Road, Riverside, CA 92507-4617, USA*

Abstract

In this study a two-dimensional numerical flow/transport model (HYDRUS-2D) was calibrated and experimentally validated using data from long furrow irrigation experiments. The model was calibrated using data from an experiment carried out assuming free-draining (FD) outlet conditions, and subsequently validated against data from three experiments assuming blocked-end conditions. The data were analyzed using the Richards' equation for variably saturated flow and either the traditional convection–dispersion equation (CDE) or the physical nonequilibrium mobile–immobile (MIM) model for solute transport. Optimization was accomplished by means of Levenberg–Marquardt optimization in combination with the HYDRUS-2D model. Simultaneous and two-step optimization approaches were used to estimate the soil hydraulic and solute transport parameters near the FD furrow inlet and outlet sites. First, the saturated hydraulic conductivity (K_s) and CDE or MIM solute transport parameters were estimated simultaneously. We also used sequential (two-step) estimation in which we first estimated the soil hydraulic parameters followed by estimation of the solute transport parameters. In the two-step method, the saturated soil water content (θ_s), the n parameter in van Genuchten's soil water retention model, and K_s values were estimated during the first step, and the CDE or MIM solute transport parameters during the second step.

Estimated soil hydraulic and solute transport parameters were found to vary substantially between the inlet and outlet sites. Estimated CDE and MIM transport parameters were very similar for both optimization approaches. The two-step method significantly improved predictions of the soil water content during model calibration, while the solute concentration predictions were nearly the same for both approaches, with both not providing a good description of the observed concentrations. Solute data were also analyzed using horizontal averages to somewhat lessen the effects of spatial variability. Horizontally averaged concentration distributions showed better agreement with the predictions. Soil water contents for the three blocked-end experiments during model validation were well predicted. The two-step method produced slightly better agreement with observed data. However, both optimization approaches produced relatively poor agreement between measured and predicted solute concentrations and deep percolation rates.

* Corresponding author. Tel.: +32-16-329756; fax: +32-16-329760.

E-mail addresses: jan.feyen@agr.kuleuven.ac.be (J. Feyen), frabbasi@hotmail.com (F. Abbasi), rvang@ussl.ars.usda.gov (M.T. van Genuchten).

[1] Tel.: +1-909-369-4847.

1. Introduction

Numerical models are increasingly being used for predicting or analyzing water flow and chemical

transport in soils and groundwater. The governing flow and transport equations are now reasonably well established, while a large number of approximate analytical or more comprehensive numerical solutions have been published during especially the last three decades. Still, a number of numerical and conceptual difficulties remain to be solved, especially for large-scale transient, multi-dimensional field applications. For example, hydrologists and engineers lack precise methodologies for identifying values of the parameters in the governing flow and transport equations. Identification and accurate simulation of field-scale processes subject to natural boundary conditions remains a complex task since many input parameters are difficult to measure at the desired scale. Recent studies (Jacques et al., 2002) indicate that a combination of numerical solutions of the governing flow and transport equations with inverse optimization algorithms and detailed measurement of different variables is a promising approach for process and parameter identification. Simultaneous estimation of the soil hydraulic and solute transport parameters from measured flow and transport data appears to be the most beneficial since the method uses cross-over effects between state variables and parameters (Sun and Yeh, 1990), and hence takes advantage of all available information. Simultaneous estimation of soil hydraulic and solute transport parameters often also yields smaller estimation errors than sequential estimation (Mishra and Parker, 1989; Šimůnek et al., 2002). Carrera and Neuman (1986) for groundwater studies similarly found that using steady-state and transient data jointly may lead to less uncertainty in many (but not all) cases, as opposed to using either type of data independently.

Notwithstanding the fact that subsurface water flow and solute transport processes have been actively studied for several decades, relatively few studies exists in which inverse methods have been used to estimate solute transport parameters using data from practical field experiments, especially when conducted during variably saturated flow. Main reasons for this are a number of practical difficulties often encountered during data collection (e.g. extreme variability of the subsurface, the time-consuming nature of many field experiments, available resources, and required labor), as well as numerical and conceptual difficulties inherent to accurately simulating field-scale solute transport. For example, one of the problems of simultaneous estimation of flow and transport parameters stems from the fact that solutions may become unstable for certain combinations of the estimated parameters (Carrera, 1987).

The main objective of this study was to estimate soil hydraulic and solute transport properties from a practical two-dimensional (2D) transient furrow irrigation experiment using simultaneous and sequential parameter optimization approaches. Optimizations were carried out using the Levenberg–Marquardt optimization in combination with the HYDRUS-2D variably saturated flow/transport software package of Šimůnek et al. (1999). The optimized parameters were subsequently used to predict water flow and solute transport in three other furrow irrigation experiments conducted at the same scale in the same field.

2. Furrow irrigation experiments

Details about the experiments can be found in Abbasi et al. (2003a,d). Only those parts of the experiments related to this study are briefly summarized here. Four large-scale furrow irrigation experiments (Fig. 1), one under free-draining (FD) and three under blocked-end conditions, were conducted at the Maricopa Agricultural Center, Phoenix, AZ, in 2001 on a bare sandy loam soil. The experiments were carried out on 115-m long furrows, spaced 1 m apart. Each experiment included three furrows, one monitored non-wheel furrow in the middle, and two guard wheel furrows, one at each side. The FD experiment was run for two successive irrigation events 10 days apart. The first irrigation lasted 275 min and the second 140 min. The average inflow rates were 1.07 and $1.03 \, l \, s^{-1}$ for the first and second irrigations, respectively. Bromide in the form of $CaBr_2$ was injected at a constant rate (6.3 g $Br \, l^{-1}$) during the entire first irrigation. The second irrigation was carried out with unamended water (without bromide) to investigate the distribution of moisture and Br in the soil profile below and adjacent to the furrow.

Two sets of neutron probe access tubes were installed at $x = 5$ and 110 m along the monitored furrow. Hereafter we refer to these locations as the inlet and outlet sites, respectively. Each set included
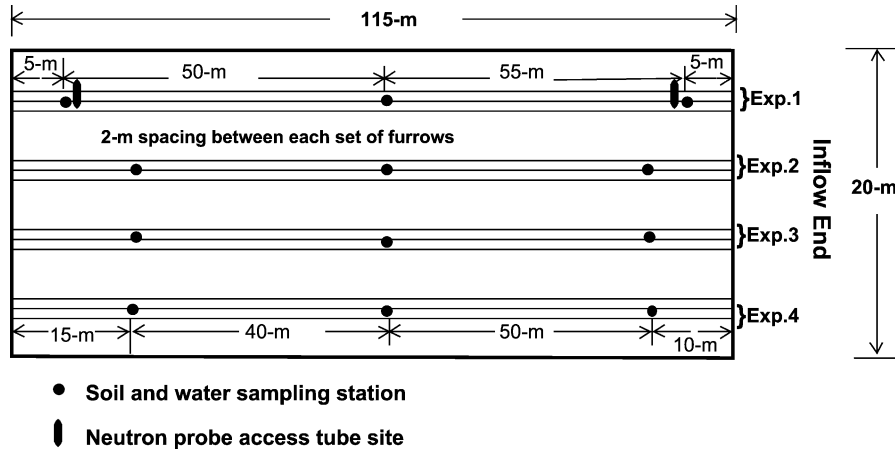
Fig. 1. Plane view of the furrow irrigation field experiments at Maricopa Agricultural Center, Phoenix, AZ (axes are not to scale).

five 2.2-m long neutron probe access tubes, installed in two rows at different locations in a cross-section perpendicular to the furrow, spaced 50 cm apart to avoid mutual interference of the readings (Fig. 2). A site-calibrated neutron probe was used for repeated measurement of the soil water content at depths of 20, 40, 60, 80, 100, 140 and 180 cm. In addition to initial readings before each irrigation event, water contents were recorded 6 and 12 h after each irrigation and then daily. Measurements were taken up to 15 days after the second irrigation. Water contents of the surface layer (0–30 cm) were also measured with Time Domain Reflectometry at the same times as neutron probe readings were taken.

Three experiments were conducted on blocked-end furrows using the following three solute application

options (referred to as the 100%, FH and SH experiments, respectively):

bromide applied during the entire irrigation (100%),
bromide applied during only the first half of the irrigation (FH),
bromide applied during the second half of the irrigation (SH).

All three experiments involved one 140-min long irrigation. The average inflow rates for the three runs were 1.29, 1.32, and 1.28 l s^{-1}, respectively. Average applied bromide concentrations for the 100%, FH, and SH experiments were 2.36, 2.79, and 5.35 g l^{-1}, respectively. We tried to apply the same amount of
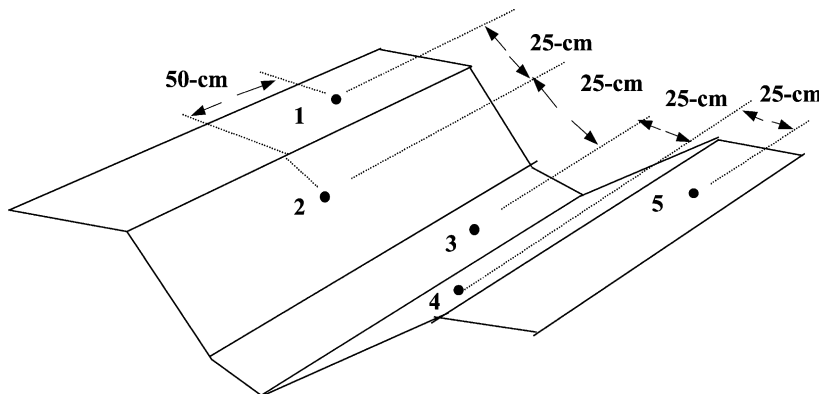

Fig. 2. Position of neutron probe access tubes at different locations in the furrow cross-section. Numbers relate to access tubes installed in two different rows; the first row includes tubes 2 and 4 along the sides and the second row includes tubes 1, 3, and 5.

solute (not the same concentration) during each experiment. However, because of several unforeseen practical problems, this objective was not fully met. Below we summarize the remaining measurements for both the FD and blocked-end experiments.

Soil samples for analyzing bromide concentrations and gravimetric soil water contents were collected five days after each irrigation at three different locations: at 10, 60 and 100 m from the inlet for the blocked-end experiments, and at 5, 60 and 110 m for the FD experiment (the inlet, middle, and outlet sites, respectively). The samples were taken from one side of the monitored furrows at three locations (top, side, and bottom of the furrows; e.g. at locations 1, 2 and 3 in Fig. 2) in a cross-section perpendicular to the furrow axis at similar depths as used for the neutron probe measurements. Soil samples from the FD experiment were also taken five days after the second irrigation. Soil water extractions (1:1 weight:volume ratios) were taken and analyzed for bromide with a Lachat QuikChem flow injection analyzer using standard colorimetric procedures. Overland water samples (for analysis of bromide concentrations) and water flow depths in the furrows were also taken at the inlet, middle, and outlet sites every few minutes as soon as water reached a particular station. Geometries of the furrows were measured with a profilometer before and after each irrigation at the inlet, middle, and outlet sites. These measured geometries served as the upper boundaries for our numerical calculations using HYDRUS-2D. We also took soil bulk densities at several locations using a Madera soil sampler up to a depth of 180 cm. In addition, 38 undisturbed soil samples (6-cm long, 5.4-cm diameter soil cores) were collected at selected locations and depths (up to 100 cm) for laboratory analyses of the soil water retention curve. The first FD irrigation was carried out on March 23, 2001, and the second irrigation 10 days later, while the 100% and FH experiments were carried out on the same day (April 3, 2001) and the SH experiment one day later. An 18-mm 3-h long rainfall event occurred on April 7.

2.1. Governing equations

The data were analyzed in terms of the Richards' equation for variably saturated flow and either the traditional convection–dispersion equation (CDE) or the physical nonequilibrium mobile–immobile (MIM) model for solute transport (van Genuchten and Wagenet, 1989; Clothier et al., 1998). Detailed descriptions of the governing equations for water flow and solute transport and the invoked parameter optimization procedure are given by Abbasi et al. (2003c).

2.2. Initial and boundary conditions

Measured bromide concentrations and soil water contents before the experiments were used as initial conditions within the flow domain. Time-space dependent flow depths (surface ponding, $h(x, t)$ in Fig. 3) and overland bromide concentrations were specified as the upper boundary condition in the furrow during irrigation, while averages of measured pan evaporation rates from the nearest weather station (about 150 m away from the experimental field) and estimated reference evapotranspiration rates obtained using the Penman–Monteith method (as reported by Abbasi et al., 2003a) were used as atmospheric boundary conditions during redistribution phase. As indicated earlier, in each experiment flow depths at the inlet, middle, and outlet sites were frequently
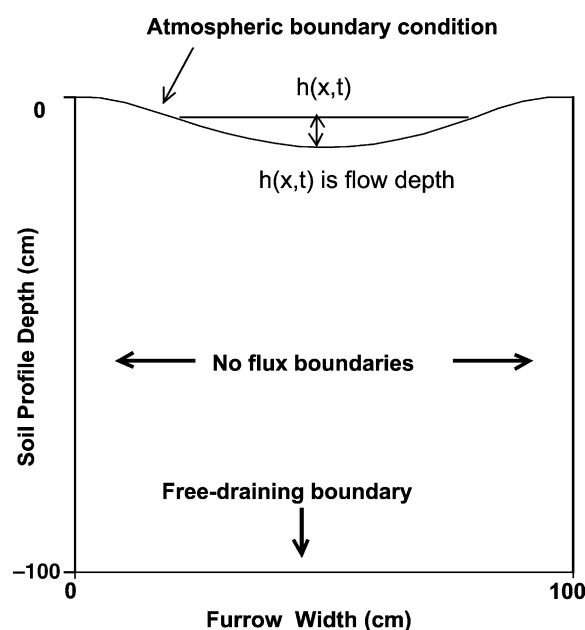

Fig. 3. Water and solute boundary conditions used for the HYDRUS-2D calculations.

measured. A Cauchy condition was used for the upper boundary condition for solute transport, while free-drainage conditions for both water and solute were applied to the lower boundary of the domain (Fig. 3). No-flux boundary conditions were applied to both sides of the flow domain. Measured furrow cross-sections were used to define the upper section of the flow domain for each experimental site. A relatively fine grid (~ 0.5 cm) was used near the soil surface, and a much coarser grid (~ 4 cm) at and near the bottom of the domain.

2.3. Parameter estimation

Soil hydraulic and CDE and MIM solute transport parameters were inversely estimated using the Levenberg–Marquardt optimization (Marquardt, 1963; Šimůnek and Hopmans, 2002) in combination with the HYDRUS-2D numerical code (Šimunek et al., 1999) using two optimization approaches. First, we estimated the saturated hydraulic conductivity (K_s) and the CDE or MIM solute transport parameters simultaneously. Of the soil hydraulic parameters only K_s was included in the optimization since we did not have any direct measurements of K_s. Also, it is generally not recommended to estimate too many parameters simultaneously because of possible corre-lation among the parameters and resulting uniqueness problems (Hopmans et al., 2002). To further improve the model predictions, a two-step optimization approach was also carried out in which we first estimated the saturated soil water content (θ_s), the parameter n in van Genuchten's soil hydraulic property model, and K_s as the most sensitive soil hydraulic parameters (Abbasi et al., 2003b), followed by estimation of transport parameters. Soil water content readings and solute concentrations were used in the objective function during the optimization process.

As indicated earlier, two sets of neutron probe access tubes at the inlet and outlet sites of the monitored furrow were available during the FD experiments for detailed water content measurements. The FD experiment hence produced relatively more information for the purpose of inversely estimating the soil hydraulic and solute transport parameters (model calibration). FD parameter estimates were subsequently used to simulate the other experiments

(model validation). In this study we assumed equivalent homogeneous soil profiles because of insufficient field data to distinguish between the different soil layers. A previous, more detailed study on short furrows (3-m long) at the same field showed that considering soil heterogeneity did not significantly improve the model predictions (Abbasi et al., 2003b).

3. Results and discussion

3.1. Estimation of soil water retention properties

The soil water retention curve, $\theta(h)$, was described using the closed-form equation of van Genuchten (1980), and the unsaturated soil hydraulic conductivity function, $K(h)$, using the statistical pore-size distri-bution model of Mualem (1976). Laboratory-measured soil water retention curves from 38 soil samples were scaled using linear scaling relationships proposed by Vogel et al. (1991) to reduce and quantify spatial variability in the soil hydraulic properties. In this study we fixed the saturated ($\theta_s^* = 0.411$ cm^3 cm^{-3}) and residual ($\theta_r^* = 0.106$ cm^3 cm^{-3}) soil water contents at the averages of the fitted local θ_s and θ_r values, while l in Mualem's equation was assumed to be 0.5 (Mualem, 1976). K_s values were inversely estimated from the measured soil water contents since no hydraulic conductivity measurements were made.

Measured (un-scaled), scaled, and reference soil water retention curves are shown in Fig. 4. The effect of scaling is clearly noticeable on the retention curves, and reflects the considerable spatial variability in the soil hydraulic properties at the field site. Scaled α and n values in van Genuchten's (1980) equation were 0.039 cm^{-1} and 1.55, respectively. The soil hydraulic parameters thus obtained (including θ_s and θ_r) were similar (except possibly α) to those estimated using neural network-based pedotransfer functions (the ROSETTA code) derived by Schaap et al. (2001). ROSETTA predicts the van Genuchten parameters and K_s in a hierarchical manner from soil textural fractions, bulk density, and one or two water retention points. Values for θ_s^*, θ_r^*, α, and n estimated with ROSETTA (assuming $l = 0.5$) were 0.407 cm^3 cm^{-3}, 0.066 cm^3 cm^{-3}, 0.055 cm^{-1}, and 1.50, respectively.
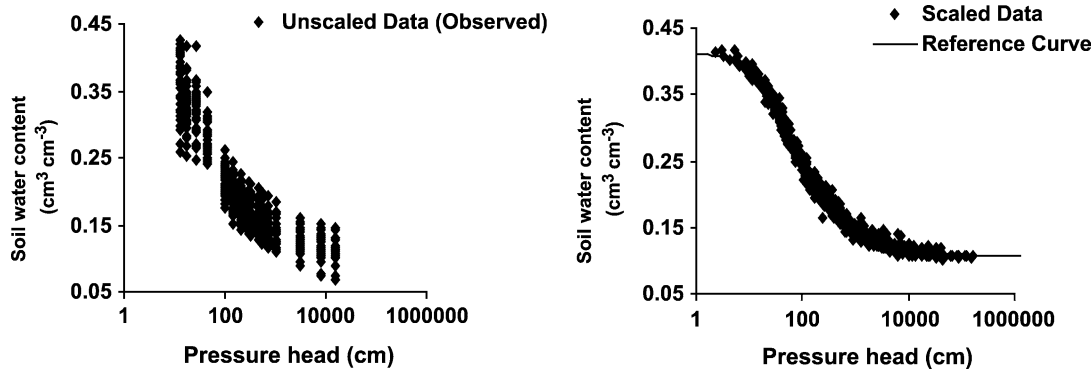
Fig. 4. Measured (un-scaled), scaled, and reference soil water retention curves.

4. Model calibration

Simultaneously optimized K_s values and CDE and MIM solute transport parameters for the inlet and outlet sites of the FD experiment are listed in Table 1. Estimated K_s values were similar for both sites along the furrow, and comparable to those estimated with the ROSETTA code (Schaap et al., 2001) as well with those obtained earlier for short furrows at the same field (Abbasi et al., 2003b,c). The K_s value estimated with ROSETTA was 0.097 cm min^{-1}.

Notice that the optimized CDE and MIM solute transport parameters (Table 1) are very similar at a given location, but differ substantially between the inlet and outlet sites. The considerable differences between the longitudinal (λ_L) and transverse (λ_T) dispersivities of the inlet and outlet sites reflect the considerable spatial variability in the soil hydraulic and transport characteristics in spite of scaling of the water retention data. This discrepancy may be partly due also to slightly different imposed flow conditions (flow depths and water and solute application times) at the two sites. The λ_L and λ_T values are comparable to

the range of values obtained for the short furrows (Abbasi et al., 2003b,c). The λ_T value for the inlet site was somewhat larger than those reported earlier for the short furrows. We believe that this is caused by more lateral water flow and solute spreading at the inlet site, which had a higher water level in the furrow and longer water and solute application times as compared to the outlet site. Also contributing to the higher λ_T value of the inlet site likely was its relatively low initial water content and the larger scale of the FD experiment. Fig. 7a and b show that lateral solute spreading was very pronounced at the inlet site. Fried (1975) and Gelhar et al. (1992), among others, showed that the dispersivity increases with the scale of observation, while studies by White et al. (1986) and Steenhuis and Muck (1988) and others showed that the initial soil water content can also have an important effect. However, the latter is in contrast to a study by Flury et al. (1994) who showed that of 14 different field sites the initial soil water content had relatively little impact at several of the sites and no effect at all at other sites. Numerical studies also showed a dependency of lateral solute spreading on

Table 1

Summary of the simultaneously optimized saturated hydraulic conductivity, K_s, and CDE and MIM solute transport parameters for the FD inlet and outlet sites

Site	K_s (cm min^{-1})	θ_{im} (cm^3 cm^{-3})	ω (min^{-1})	λ_L (cm)	λ_T (cm)	SSQ (−)	R^2 (−)
Inlet	0.0835 (0.0847)	0.030	0.028	22.2 (24.2)	4.4 (4.2)	5.975 (5.797)	0.829 (0.828)
Outlet	0.0953 (0.0945)	0.045	0.020	9.1 (9.2)	0.01 (0.07)	1.413 (1.328)	0.849 (0.847)
Average[a]	0.0892 (0.0895)	0.0367	0.024	14.3 (14.9)	0.21 (0.54)	–	–

Optimized values for the CDE runs are given in parentheses.

[a] Geometric average of estimated parameters for the inlet and outlet sites used for model validation.

Table 2a
Summary of optimized soil hydraulic parameters during the first step of the sequential (two-step) parameter estimation method

Site	n (–)	θ_s (cm^3 cm^{-3})	K_s (cm min^{-1})	SSQ (–)	R^2 (–)
Inlet	1.53	0.301	0.0424	0.317	0.733
Outlet	1.31	0.387	0.1066	0.795	0.315
Average[a]	1.41	0.341	0.0679	–	–

[a] Geometric average of estimated parameters for the inlet and outlet sites used for model validation.

the initial soil water content between and below the furrows (Abbasi, 2003).

Similar to the small-scale experiments of Abbasi et al. (2003c), the FD experiment revealed relatively low immobile water contents (θ_{im}), thus indicating that advection and dispersion were the main transport processes in this study. Estimated first-order exchange coefficients (ω) were generally somewhat lower than those obtained for the small-scale experiments, but comparable with those reported in the literature for one-dimensional (1D) water flow and solute transport studies (Nkedi-Kizza et al., 1983; Seyfried and Rao, 1987; Maraqa et al., 1999; among others).

Estimated soil hydraulic and solute transport parameters using the sequential (two-step) optimization method are given in Table 2. Notice that the sum of the squared residuals (SSQ) are much lower than those obtained with the simultaneous approach. However, the R^2 values for the two-step method are generally lower than those for the simultaneous approach. The soil hydraulic parameters (Table 2a) are consistent with those obtained earlier for the short furrows (Abbasi et al., 2003b). The value of n is also comparable with laboratory-measured values, as well as with those estimated with ROSETTA, while θ_s values are somewhat smaller than those estimated with ROSETTA and measured in the laboratory on small

soil samples. Estimated K_s values differed considerably between the inlet and outlet sites, and were lower/higher than those obtained with simultaneous optimization method (Table 1). However, they are still within range of estimated values obtained for the short furrows.

Estimated solute transport parameters (Table 2b) for the CDE and MIM models were again similar; however, they varied substantially between the two sites. Since they produced very similar results, the CDE model is preferred because it has fewer parameters, is less vulnerable to parameter uniqueness problems, and requires less computational time. The estimated θ_{im} and ω values for the inlet site were substantially larger than those for the outlet site and those estimated using the simultaneous optimization method (Table 1). The λ_L and λ_T parameter values differed also considerable for the two sites. Overall, estimated λ_L values using the simultaneous and two-step approaches for both inlet and outlet sites of the FD experiment were consistent with those obtained for the short furrow experiments assuming homogeneous soil profiles (Abbasi et al., 2003c), but somewhat lower than those estimated for the same experiments assuming layered profiles (Abbasi et al., 2003b). Discrepancies between the estimated parameters for the long FD experiment and the short furrows may be due to the inherent spatial variability in the soil hydraulic and solute transport properties, and partly due to the imposed flow conditions (flow depths and water and solute application times).

Measured soil water contents and solute concentration values for both the inlet and outlet sites are compared in Fig. 5 with the predicted values. Two-step optimization produced better agreement with the observed water contents, whereas solute concentrations obtained with both optimization methods were more or less the same, with both of them giving

Table 2b
Summary of optimized solute transport parameters during the second step of the sequential (two-step) parameter estimation method

Site	θ_{im} (cm^3 cm^{-3})	ω (min^{-1})	λ_L (cm)	λ_T (cm)	SSQ (–)	R^2 (–)
Inlet	0.10	0.3475	20.05 (19.85)	4.34 (4.34)	0.308 (0.308)	0.703 (0.702)
Outlet	0.036	0.0314	1.74 (1.84)	0.04 (0.03)	0.159 (0.159)	0.850 (0.849)
Average[a]	0.06	0.1045	5.91 (6.04)	0.422 (0.36)	–	–

Optimized values for the CDE runs are given in parentheses.
[a] Geometric average of estimated parameters for the inlet and outlet sites used for model validation.

relatively poor descriptions of the data. Notice that the R^2 values in Fig. 5 represent regression of measured versus predicted results for the inlet and outlet sites whereas the R^2 values given in Tables 1 and 2 hold for specific data types used in the individual inlet and outlet optimizations.

Measured and calibrated (using the simultaneous and two-step optimization approaches) soil water contents and solute concentrations at the inlet and outlet sites of the FD experiment are presented in Figs. 6 and 7. Results are given by means of 1D curves to provide a better visual comparison between the measured and calculated distributions. Results are given at two different times (12 h and five days after the first irrigation, being representatives of relatively wet and dry conditions, for soil water contents and five days after each irrigation for concentrations) and for three different locations in the furrow cross-section (bottom, side and top of the furrow) up to a depth of 100 cm below the soil surface. Results are plotted versus depth (instead of versus lateral distance) since considerable more data were available

versus depth. The CDE and MIM model simulations were always very similar (Tables 1 and 2). For this reason, for both model calibration and validation, we are showing here only results obtained with the CDE transport model.

The simultaneous optimization approach overestimated soil water contents of the different inlet sampling locations (Fig. 6a and b). We believe that hysteresis, which often occurs in field-scale studies, and air entrapment, may have played a major role in this study since the calculated water contents immediately after each irrigation quickly reached saturation ($\theta_s = 0.411$ cm^3 cm^{-3} as measured on small soil samples in the laboratory) in almost the entire soil profile. By comparison, the maximum measured water content was only about 0.34 cm^3 cm^{-3} (about 83% of θ_s), which occurred in the surface layer below the furrow bottom (results not further shown here). These results agree with findings by Klute (1986), among others, who showed that field-measured θ_s values are often much lower than the porosity because of entrapped or dissolved air. Using laboratory
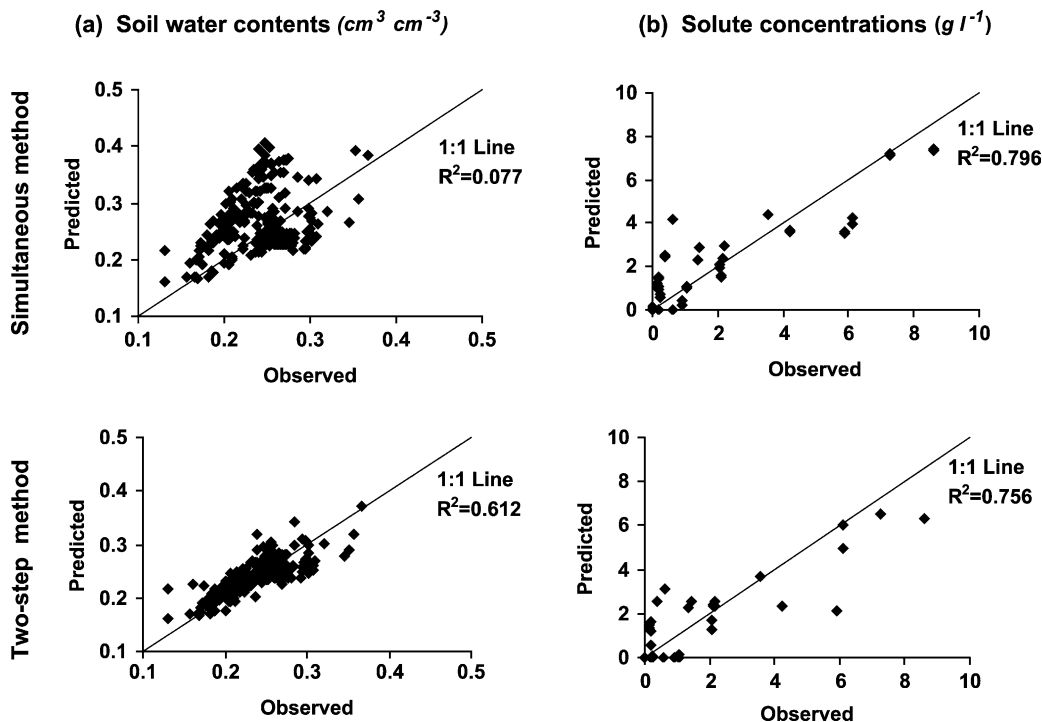

Fig. 5. Measured versus predicted (using simultaneous and two-step parameter optimizations) soil water contents and solute concentrations (for both the CDE and MIM models) for the inlet and outlet sites of the free-draining experiment.
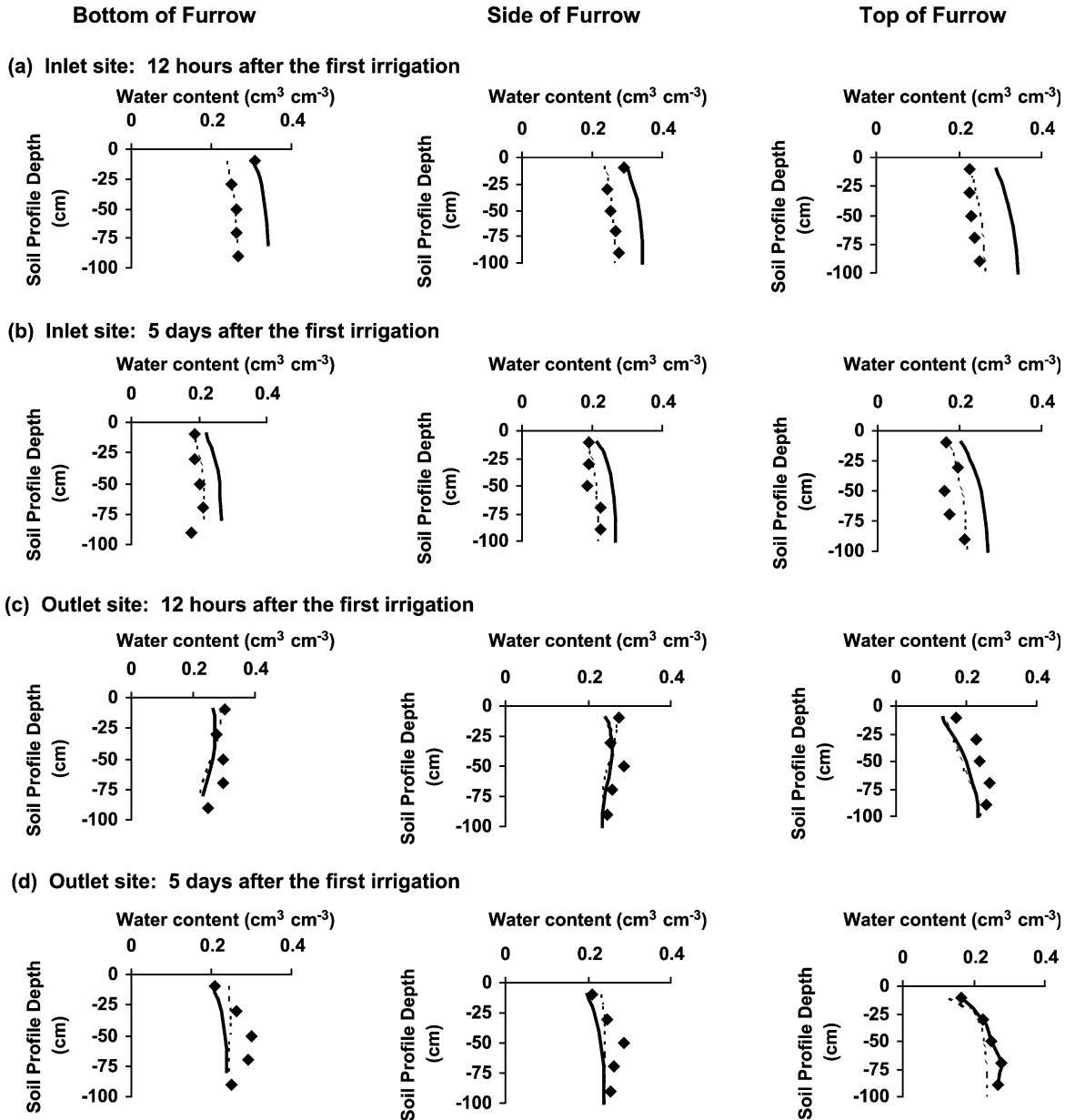
Fig. 6. Measured and calibrated (using simultaneous and two-step parameter optimizations) soil water contents for the inlet and outlet sites of the free-draining experiment (measured: symbols, simultaneous: solid lines, two-step: dashed lines).

estimated soil water retention parameters to describe soil water status at the field scale is another possible reason for the discrepancy between the measured and simulated soil water contents using the simultaneous parameter estimation approach. Estimation

and application of soil hydraulic properties should be made in the same scale. Agreement between measured and calculated water contents was much better for the outlet site than the inlet site (Fig. 6c and d). Hysteresis likely was far less important at the outlet site because

Bottom of Furrow　　**Side of Furrow**　　**Top of Furrow**

(a) Inlet site: 5 days after the first irrigation

(b) Inlet site: 5 days after the second irrigation

(c) Outlet site: 5 days after the first irrigation

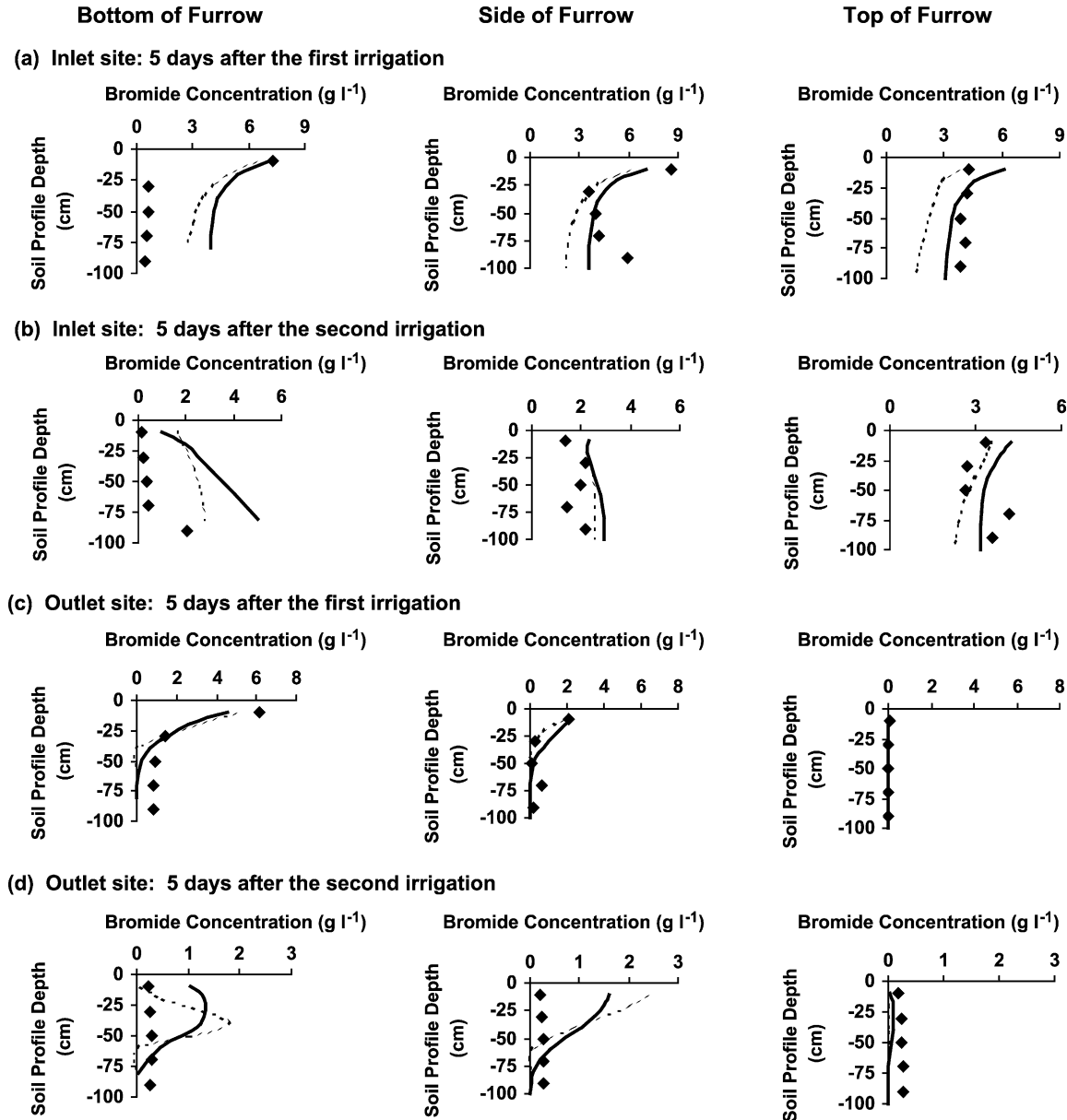**(d) Outlet site: 5 days after the second irrigation**

Fig. 7. Measured and calibrated (using simultaneous and two-step parameter optimizations, and the CDE solute transport model) bromide concentrations for the inlet and outlet sites of the free-draining experiment at different times (measured: symbols, simultaneous: solid lines, two-step: dashed lines).

of shorter water and solute application (opportunity) times, which caused predicted water contents never to reach θ_s. For instance, opportunity times for the inlet and outlet sites during the first irrigation were 300 and 63 min, respectively. Our data were not sufficient to take into account the hysteresis.

Simulations obtained using the two-step method were satisfactory compared to the simultaneous optimization approach. This was expected since more hydraulic parameters were optimized with the two-step method (in particular θ_s). Agreement between measured and simulated soil water contents during

the second irrigation was more or less the same as for the first irrigation (results not further shown here).

Overall, agreement between measured and calculated solute concentrations (Fig. 7) was less satisfactory, likely because of spatial and temporal variability in the soil hydraulic and solute transport properties. Temporal variability was caused by physical deterioration of the furrow surface during the two irrigation events. Both optimization methods produced poor results at several locations (Fig. 7a and b; bottom of the furrow, and Fig. 7d; bottom and side of the furrow), but better agreement with the data in other cases (Fig. 7c; all locations).

As noted earlier, flow and solute transport parameters can display substantial spatial and temporal variations that are difficult to characterize since perfect knowledge about the variations is generally impossible to acquire. Many methods, often for saturated media, have been employed to approximate spatial distributions, such as zonation, pilot points,

splines, and finite elements (Yeh, 1986; Carrera, 1987). In a recent transient study, Forrer et al. (1999) processed their 2D solute distributions by means of horizontal and vertical averaging to reduce spatial variability and produce 1D concentration profiles for comparisons with model predictions. They found that horizontally averaged solute distributions were much smoother than vertically averaged distributions.

To further lessen the effects of spatial variability (in addition to scaling of the soil water retention data), solute concentration data were subjected to horizontal and vertical averaging. Horizontal averages of the measured and predicted bromide concentrations for the different FD sampling sites are shown in Fig. 8. Following Forrer et al. (1999), we used simple arithmetic averaging. Vertically averaged results are not presented because of limited data at each site (only three points were available). Horizontal averaging significantly improved agreement between measured and model predictions for the first irrigation of the FD
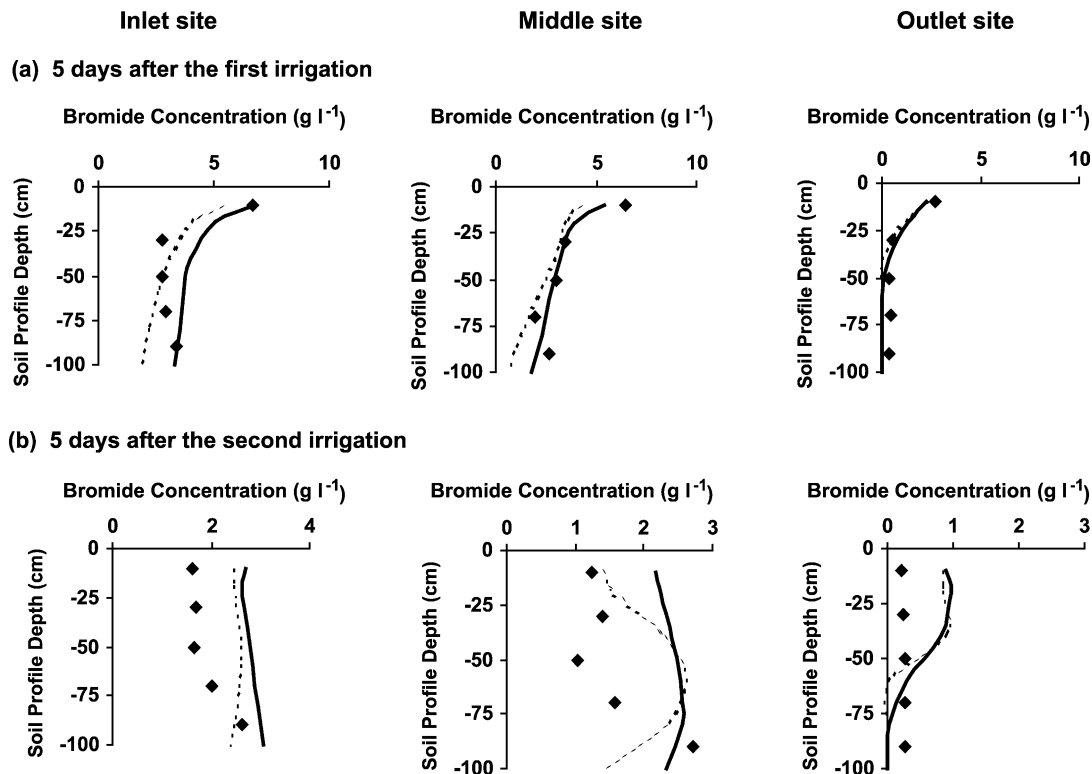

Fig. 8. Horizontally averages of measured and calibrated (using simultaneous and two-step parameter optimizations, and the CDE solute transport model) bromide concentrations for the different sites of the free-draining experiment (measured: symbols, simultaneous: solid lines, two-step: dashed lines).

experiment (Fig. 8). However, the expected improvement was not achieved for the second irrigation (five days after the second irrigation). Note that results for the FD middle sites, predicted by geometric means of the obtained values for the inlet and outlet sites given in Tables 1 and 2, were also included in Fig. 8.

5. Model validation

Optimized soil hydraulic and CDE solute transport parameters obtained with the simultaneous and two-step optimization methods from the FD experiment

were used to experimentally test (validate) the HYDRUS-2D model for the other three experiments. For this purpose, we used geometric averages of the optimized parameters from the inlet and outlet sites of the FD experiment (Tables 1 and 2) to predict soil water contents, solute concentrations, and deep percolation rates of water and solutes from the 100%, FH, and SH experiments. Horizontally averaged solute concentrations were presented because of large spatial variability between the different sites in the furrow cross-section.

Measured and simulated soil water contents of the different sites (inlet, middle, and outlet) of the 100%
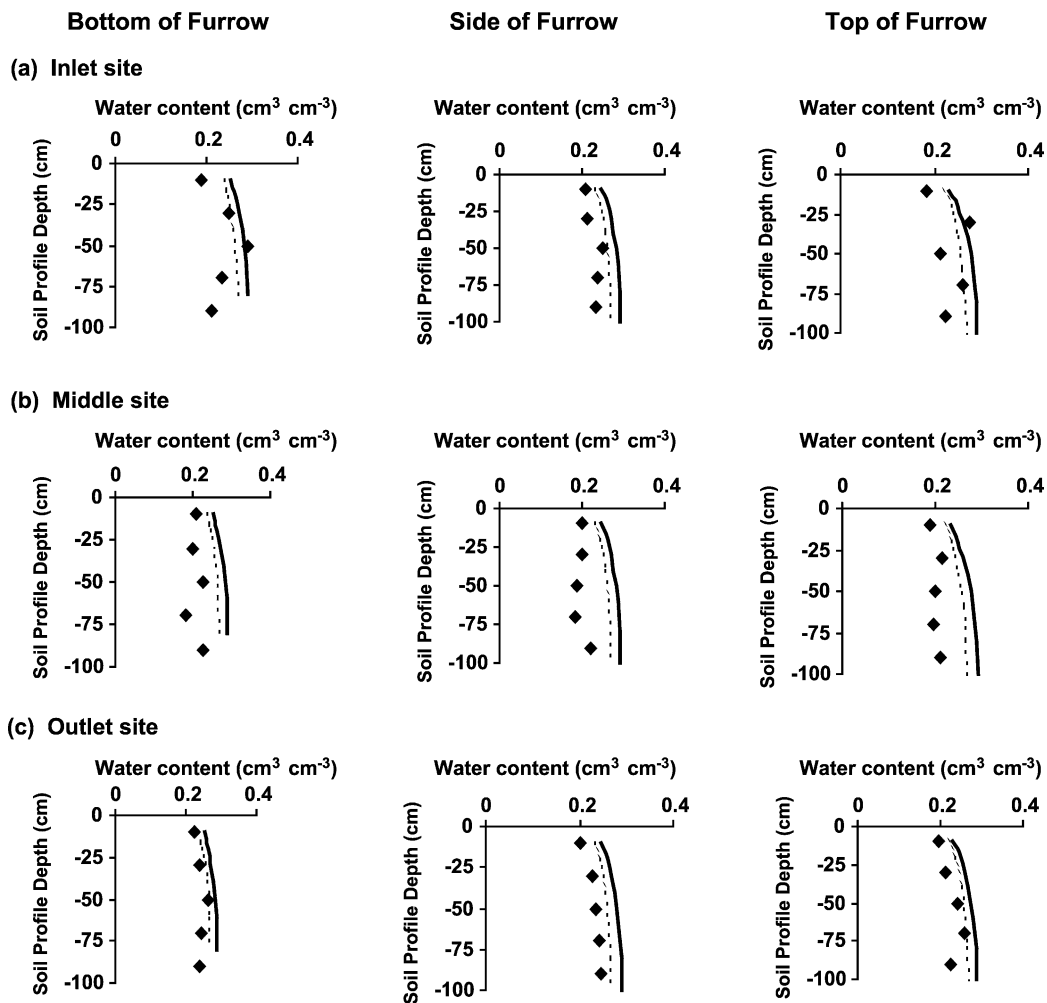

Fig. 9. Measured and predicted (using simultaneous and two-step parameter optimizations) soil water contents for the different sites of the 100% experiment, five days after irrigation (measured: symbols, simultaneous: solid lines, two-step: dashed lines).

experiment are compared in Fig. 9. Despite considerable variability and uncertainty in the soil hydraulic parameters, typical of field-scale studies, agreement between measured and predicted soil water contents was relatively good. Similar to model calibration, the two-step optimization approach produced better predictions with the measured values. Discrepancies in some cases (Fig. 9b) were due to the some of the factors discussed under model calibration (e.g. hysteresis and variability in the soil hydraulic

properties). Results for the FH and SH experiments were more or less like 100% experiment (not further shown here).

Neither the simultaneous nor the two-step optimization methods described the solute concentrations well. Concentrations were overestimated at some of the sites (Fig. 10a, middle and outlet sites). We believe that this was mostly due to having insufficient data for the optimization procedure to accurately estimate the transport parameters, and because of
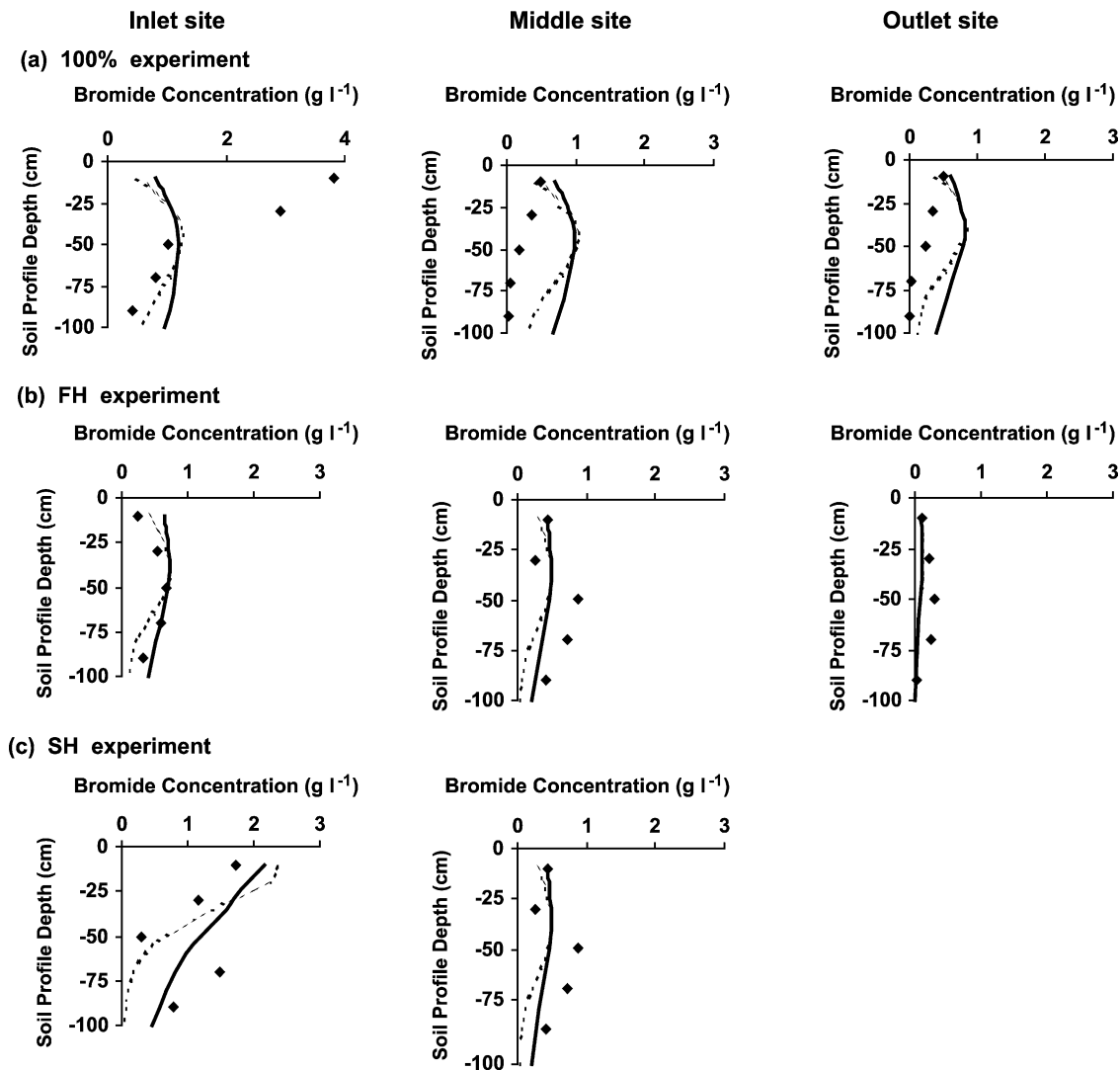

Fig. 10. Horizontally averages of measured and predicted (using simultaneous and two-step parameter optimizations, and the CDE solute transport model) bromide concentrations for the different sites of the 100%, FH, and SH experiments, five days after irrigation (measured: symbols, simultaneous: solid lines, two-step: dashed lines). Note that water did not reach the end in the SH experiment.

Table 3
Measured and predicted (using the simultaneous and two-step parameter optimization methods and the CDE solute transport model) deep percolation rates of water and solutes at the different sites of the various experiments

Experiment	Measured		Predicted (simultaneous)		Predicted (two-step)	
	Water (l/m)	Solute (g/m)	Water (l/m)	Solute (g/m)	Water (l/m)	Solute (g/m)
FD						
Inlet	82.7	139.7	129.2	382.5	65.1	101.0
Middle	50.2	95.9	126.0	363.6	39.4	30.9
Outlet	24.1	8.4	5.9	0.0	4.6	0.0
100%						
Inlet	57.0	13.0	91.4	78.7	68.9	31.7
Middle	71.6	3.2	49.7	31.2	39.5	10.1
Outlet	46.6	1.1	22.2	8.7	19.6	2.1
FH						
Inlet	68.6	16.1	28.9	11.8	10.7	1.1
Middle	66.9	11.2	18.3	4.2	4.8	1.1
Outlet	45.9	0.7	1.6	0.0	0.0	0.0
SH						
Inlet	40.3	23.0	34.4	16.0	14.1	0.4
Middle	23.6	5.8	2.9	0.5	0.0	0.0

averaging of the optimized transport parameters obtained from the inlet and outlet sites (which showed relatively large differences in dispersivities; see Tables 1 and 2). Also, point measurements often lead to poor representations of water flow and transport behavior at field scale (Tsang et al., 1996). Point measurements additionally can cause considerable underestimation of chemical fluxes as shown by Ritsema and Dekker (1996), and generally involve uncertainties induced by human, instrumental, and hydrogeological errors (Xiang et al., 1992). Both optimization methods predicted the concentrations near the soil surface relatively well, except for the inlet site of the 100% experiment where they were underestimated. Notice that the irrigation water in the furrow never reached the end of the SH experiment because of high infiltration and roughness properties.

Measured and predicted deep percolation rates for water (WDP) and solute (SDP) five days after irrigation are presented in Table 3. WDP and SDP are defined as the amounts of water and solute, respectively, percolating below a depth of 100 cm. In order to calculate WDP and SDP, soil profiles below the depth of 100 cm down to 180 cm were divided into a network of rectangular elements, each being approximately 25 cm by 30 cm. Volumes of water and masses of bromide were determined for each rectangle, and then summed to obtain the total amounts of water/bromide. We used for this purpose measured gravimetric soil water contents, soil bulk densities, and bromide concentrations at different depths.

Deep percolation rates of water and solutes were overestimated/underestimated for the various experiments (Table 3). The simultaneous approach
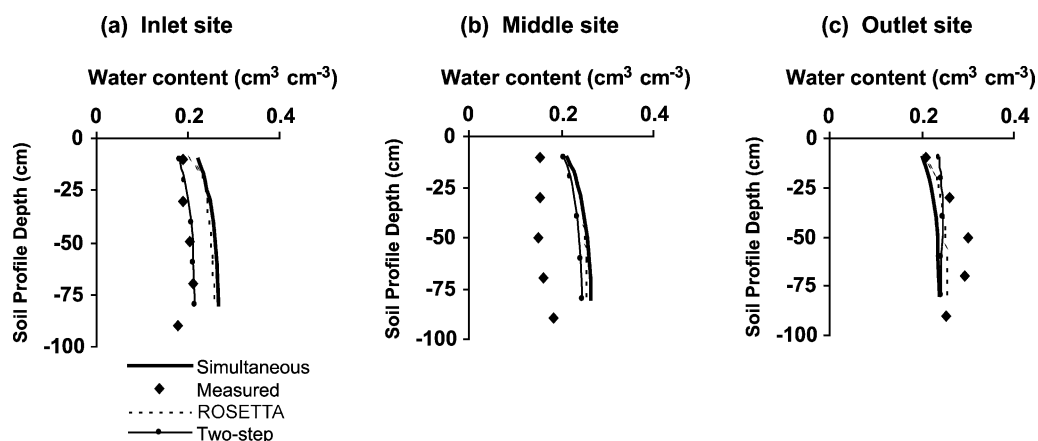

Fig. 11. Measured and predicted (using simultaneous and two-step parameter optimizations, and the ROSETTA code) soil water contents at the bottom of the inlet, middle, and outlet sites of the free-draining experiment, five days after the first irrigation.

overestimated the rates for the inlet and middle sites of the FD experiment, while the two-step method predicted the values somewhat better for those sites. However, both methods underestimated the rates for the outlet site. Both optimization approaches underestimated deep percolation rates of water and solutes for the different sites of the various blocked-end experiments, except those estimated with the simultaneous method for the inlet site of the 100% experiment. The two-step predictions were slightly better for the inlet site of the 100% experiment, whereas the simultaneous predictions were somewhat better for other sites. The rates for the FH and SH experiments were also predicted somewhat better with the simultaneous approach.

Finally, we compared predicted soil water content distributions obtained using the simultaneous and two-step optimization methods, against predictions using pedotransfer functions obtained with the ROSETTA code of Schaap et al. (2001). Essentially the same water content distributions were obtained with ROSETTA and the two optimization approaches, exemplified by the plots in Fig. 11. This shows that ROSETTA can be a relatively fast, easy, and cost-effective method for estimating soil hydraulic properties, as compared to using direct measurement methods.

6. Conclusions

In this study we calibrated and experimentally tested (validated) the HYDRUS-2D numerical code against four real furrow irrigation experiments. The soil hydraulic and solute transport parameters were estimated using simultaneous and sequential optimization of data from two sites near the inlet and outlet sites of a FD furrow experiment assuming homogeneous soil profiles. The optimized parameters were subsequently used for model validation to produce soil water contents and solute concentrations in three other blocked-end furrow experiments conducted in the same field.

The optimized parameters were very similar to those reported earlier for short furrows at the same experimental site. Minor differences were related to the presence of soil heterogeneity across the field and versus depth, different observation scales, and different imposed flow conditions (flow depths and water and solute applications times). Optimization resulted in similar parameters for the CDE and MIM transport models. In spite of scaling of the laboratory-measured soil water retention data, estimated parameters along the monitored furrow, particularly the longitudinal and transverse dispersivities, were found to be vary spatially because of inherently different soil properties and differently imposed flow and solute transport boundary conditions (e.g. varying flow depths, and irrigation and solute application times). Agreement between measured and predicted soil water contents was satisfactory with the sequential optimization approach whereas the simultaneous method overestimated the soil water contents. Observed solute concentrations along the furrow cross-sections displayed more spatial variability than the soil water contents and were not predicted as well as the soil water contents. Spatial averaging across the furrow cross-sections somewhat improved agreement between observed and calculated solute concentrations. Both optimization approaches predicted the solute concentrations near the soil surface reasonably well. Deep percolation rates of water and solutes were overestimated/underestimated with the simultaneous method, and underestimated with the sequential approach. Two-step optimization produced better agreement between predicted and measured soil water contents, but required more computational time as compared to simultaneous optimization.

This study provides further evidence that the unsaturated soil hydraulic properties should be estimated and used in model predictions at the same scale. Estimated soil hydraulic parameters from small soil cores in the laboratory may not adequately describe field-scale soil water status in view of considerable variability, uncertainty, and a number of experimental complications (especially air entrapment and macropore flow). Also, considering temporal variability in the soil hydraulic and transport parameters could well improve the model predictions further.

Acknowledgements

References

Abbasi, F., 2003. Field-scale analyses of water flow and solute transport in furrows. PhD Thesis, No. 555, K.U. Leuven, Fac. Landbouwkundige en Toegepaste Biologische Wetenschappen, Leuven, Belgium.

Abbasi, F., Feyen, J., Roth, R.L., Sheedy, M., van Genuchten, M.Th., 2003a. Water flow and solute transport in furrow-irrigated fields. Irrig. Sci. 22 (2), 57–65.

Abbasi, F., Jacques, D., Šimůnek, J., Feyen, J., van Genuchten, M.Th., 2003b. Inverse estimation of the soil hydraulic and solute transport parameters from transient field experiments: heterogeneous soil. Trans. ASAE 46 (4), 1097–1111.

Abbasi, F., Šimůnek, J., Feyen, J., van Genuchten, M.Th., Shouse, P.J., 2003c. Simultaneous inverse estimation of the soil hydraulic and solute transport parameters from transient field experiments: homogeneous soil. Trans. ASAE 46 (4), 1085–1095.

Abbasi, F., Šimůnek, J., van Genuchten, M.Th., Feyen, J., Adamsen, F.J., Hunsaker, D.J., Strelkoff, T.S., Shouse, P., 2003d. Overland water flow and solute transport: model development and field data analysis. J. Irrig. Drain. Engng 129 (2), 71–81.

Carrera, J., 1987. State of the art of the inverse problem applied to the flow and solute transport equation, in analytical and numerical groundwater flow and quality modelling. In: Custodio, E., et al. (Eds.), NATO-ARW Series C: Mathematical and Physical Sciences, vol. 224. Reidel, Norwell, Mass, pp. 549–583.

Carrera, J., Neuman, S.P., 1986. Estimation of aquifer parameters under transient and steady-state conditions: application to synthetic and field data. Water Resour. Res. 22 (2), 228–242.

Clothier, B.E., Vogeler, I., Green, S.R., Scotter, D.R., 1998. Transport in unsaturated soil: aggregates, macropores, and exchange. In: Selim, H.M., Ma, L. (Eds.), Physical Nonequilibrium in Soils: Modeling and Application, Ann Arbor Press, Chelsea, MI, pp. 273–295.

Flury, M., Fluhler, H., Jury, W.A., Leuenberger, J., 1954. Susceptibility of soils to preferential flow of water: a field study. Water Resour. Res. 30, 1945–1954.

Forrer, I., Kasteel, R., Flury, M., Fluhler, H., 1999. Longitudinal and lateral dispersion in an unsaturated field soil. Water Resour. Res. 35, 3049–3060.

Fried, J.J., 1975. Groundwater Pollution. Elsevier, New York.

Gelhar, L.W., Welty, C., Rehfeldt, K.R., 1974. A critical review of data on field-scale dispersion in aquifers. Water Resour. Res. 28 (7), 1955–1955.

van Genuchten, M.Th., 1980. A closed-form equation for predicting the hydraulic conductivity of unsaturated soils. Soil Sci. Soc. Am. J. 44, 892–898.

van Genuchten, M.Th., Wagenet, R.J., 1989. Two site/two region models for pesticide transport and degradation: theoretical development and analytical solutions. Soil Sci. Soc. Am. J. 53 (5), 1303–1310.

Hopmans, J.W., Šimůnek, J., Romano, N., Durner, W., 2002. Inverse methods. In: Dane, J.H., Topp, G.C. (Eds.), Methods of Soil Analysis. Part 4. Physical Methods, SSSA Book Series 5, Soil Science Society of America, Madison, WI, pp. 963–1008.

Jacques, D., Šimůnek, J., Timmerman, A., Feyen, J., 2002. Calibration of Richards' and convection–dispersion equations to field-scale water flow and solute transport under rainfall conditions. J. Hydrol. 259, 15–31.

Klute, A., 1986. Water retention: laboratory methods. In: Klute, A., (Ed.), Methods of Soil Analysis. Part 1. Physical and Mineralogical Methods, 2nd ed., Agronomy, 9(1). American Society of Agronomy, Madison, WI, pp. 635–662.

Maraqa, M.A., Wallace, R.B., Voice, T.C., 1999. Effects of residence time and degree of water saturation on sorption nonequilibrium parameters. J. Contam. Hydrol. 36, 53–72.

Marquardt, D.W., 1963. An algorithm for least squares estimation of non-linear parameters. J. Ind. Appl. Math. 11, 431–441.

Mishra, S., Parker, J.C., 1989. Parameter estimation for coupled unsaturated flow and transport. Water Resour. Res. 25 (3), 385–396.

Mualem, Y., 1976. A new model for predicting the hydraulic conductivity of unsaturated porous media. Water Resour. Res. 12 (3), 513–522.

Nkedi-Kizza, P., Biggar, J.W., van Genuchten, M.Th., Wierenga, P.J., Selim, H.M., Davidson, J.M., Nielsen, D.R., 1983. Modeling tritium and chloride36 transport through an aggregated oxisol. Water Resour. Res. 19, 691–700.

Ritsema, C.J., Dekker, L.W., 1996. Influence of sampling strategy on detecting preferential flow paths in water-repellent sand. J. Hydrol. 177, 33–45.

Schaap, M.G., Leij, F.J., van Genuchten, M.Th., 2001. ROSETTA: a computer program for estimating soil hydraulic parameters with hierarchical pedotransfer functions. J. Hydrol. 251, 163–176.

Seyfried, M.S., Rao, P.S.C., 1987. Solute transport in undisturbed columns of an aggregated tropical soil: preferential flow effects. Soil Sci. Soc. Am. J. 51, 1434–1444.

Šimůnek, J., Hopmans, J.W., 2002. Parameter estimation and nonlinear fitting. In: Dane, J.H., Topp, G.C. (Eds.), Methods of Soil Analysis. Part 4. Physical Methods, SSSA Book Series 5, Soil Science Society of America, Madison, WI, pp. 139–157.

Šimůnek, J., Sejna, M.Th., van Genuchten, M., 1999. The HYDRUS-2D Software Package for Simulating the Two-dimensional Movement of Water, Heat, and Multiple Solutes in Variably Saturated Media, Version 2.0, IGWMC-TPS-70, International Ground Water Modeling Center, Colorado School of Mines, Golden Colorado.

Šimůnek, J., van Genuchten, M.Th., Jacques, D., Hopmans, J.W., Inoue, M., Flury, M., 2002. Solute transport during variably-saturated flow: inverse methods. In: Dane, J.H., Topp, G.C.

(Eds.), Methods of Soil Analysis. Part 4. Physical Methods, SSSA Book Series 5, Soil Science Society of America, Madison, WI, pp. 1435–1449.

Steenhuis, T.S., Muck, R.E., 1988. Preferred movement of nonadsorbed chemicals on wet, shallow, sloping soils. J. Environ. Qlty 17 (3), 376–384.

Sun, N.Z., Yeh, W.W.G., 1990. Coupled inverse problems in groundwater modeling. 1. Sensitivity analysis and parameter identification. Water. Resour. Res. 26 (10), 2507–2525.

Tsang, Y.W., Tsang, C.F., Hale, F.V., Dverstorp, B., 1996. Tracer transport in a stochastic continuum model of fractured media. Water Resour. Res. 32 (10), 3077–3092.

Vogel, T., Cislerova, M., Hopmans, J.W., 1991. Porous media with linearly variable hydraulic properties. Water Resour. Res. 27, 2735–2741.

White, R.E., Dyson, J.S., Gerstl, Z., Yaron, B., 1986. Leaching of herbicides through undisturbed cores of a structured clay soil. Soil Sci. Soc. Am. J. 50, 277–283.

Xiang, Y., Sykes, F., Thomson, N.R., 1992. A composite L_1 parameter estimator for model fitting in groundwater flow and solute transport simulation. Water Resour. Res. 29 (6), 1661–1673.

Yeh, W.W.-G., 1986. Review of parameter identification procedures in groundwater hydrology: the inverse problem. Water Resour. Res. 22 (2), 95–108.